



HAL
open science

Sustainable Activated Carbon from Agricultural Waste: A Study on Adsorption Efficiency for Humic Acid and Methyl Orange Dyes

Zahia Tigrine, Ouassila Benhabiles, Leila Merabti, Nadia Chekir, Mounir Mellal, Salaheddine Aoudj, Nora Amele Abdeslam, Djilali Tassalit, Seif El Islam Lebouachera, Nadjib Drouiche

► **To cite this version:**

Zahia Tigrine, Ouassila Benhabiles, Leila Merabti, Nadia Chekir, Mounir Mellal, et al.. Sustainable Activated Carbon from Agricultural Waste: A Study on Adsorption Efficiency for Humic Acid and Methyl Orange Dyes. Sustainability, 2024, 16 (21), pp.9308. 10.3390/su16219308 . hal-04787845

HAL Id: hal-04787845

<https://univ-pau.hal.science/hal-04787845v1>

Submitted on 18 Nov 2024

HAL is a multi-disciplinary open access archive for the deposit and dissemination of scientific research documents, whether they are published or not. The documents may come from teaching and research institutions in France or abroad, or from public or private research centers.



L'archive ouverte pluridisciplinaire **HAL**, est destinée au dépôt et à la diffusion de documents scientifiques de niveau recherche, publiés ou non, émanant des établissements d'enseignement et de recherche français ou étrangers, des laboratoires publics ou privés.



Distributed under a Creative Commons Attribution 4.0 International License

Article

Sustainable Activated Carbon from Agricultural Waste: A Study on Adsorption Efficiency for Humic Acid and Methyl Orange Dyes

Zahia Tigrine ¹, Ouassila Benhabiles ¹, Leila Merabti ¹, Nadia Chekir ², Mounir Mellal ², Salaheddine Aoudj ³, Nora Amele Abdeslam ⁴ , Djilali Tassalit ¹, Seif El Islam Lebouchera ^{5,*}  and Nadjib Drouiche ⁶

- ¹ Unité de Développement des Equipements Solaires (UDES), Centre de Développement des Energies Renouvelables (CDER), Route Nationale N°11, Bou-Ismaïl 42415, Algeria; z.tigrine@udes.dz (Z.T.); o.benhabiles@udes.dz (O.B.); l.merabti@udes.dz (L.M.); d.tassalit@mesrs.dz (D.T.)
- ² Faculty of Mechanical Engineering and Process Engineering, University of Science and Technology Houari Boumediene, BP 32, El Alia, Bab Ezzouar, Alger 16111, Algeria; nchekir@usthb.dz (N.C.); mmellal@usthb.dz (M.M.)
- ³ Faculty of Mechanical Engineering and Process Engineering, University of Blida 1 Saad Dahleb, Blida 09000, Algeria; salaheddine_aoudj@univ-blida.dz
- ⁴ Department of Physics, Faculty of Exact Sciences, University of Mohamed Khider-Biskra, Biskra 07000, Algeria; noura.abdeslam@univ-biskra.dz
- ⁵ Institut des Sciences Analytiques et de Physico-Chimie Pour L'Environnement et les Matériaux, IPREM, UMR 5254, CNRS Université de Pau et des Pays de L'Adour/E2S, 2 Avenue P. Angot, Technopôle HélioParc, 64000 Pau, France
- ⁶ Division CCSM, Centre de Recherche en Technologie Semi-Conducteurs Pour L'Energétique, N2, Bd Frantz Fanon, Alger Sept Merveilles, Alger 16038, Algeria; drouichenadjib@crtse.dz
- * Correspondence: s.lebouchera@univ-pau.fr



Citation: Tigrine, Z.; Benhabiles, O.; Merabti, L.; Chekir, N.; Mellal, M.; Aoudj, S.; Abdeslam, N.A.; Tassalit, D.; Lebouchera, S.E.I.; Drouiche, N. Sustainable Activated Carbon from Agricultural Waste: A Study on Adsorption Efficiency for Humic Acid and Methyl Orange Dyes.

Sustainability **2024**, *16*, 9308.

<https://doi.org/10.3390/su16219308>

Academic Editor: Kaan Yetilmezsoy

Received: 24 September 2024

Revised: 19 October 2024

Accepted: 22 October 2024

Published: 26 October 2024



Copyright: © 2024 by the authors. Licensee MDPI, Basel, Switzerland. This article is an open access article distributed under the terms and conditions of the Creative Commons Attribution (CC BY) license (<https://creativecommons.org/licenses/by/4.0/>).

Abstract: In this study, porous activated carbon was produced from coffee waste and used as an effective adsorbent for the removal of humic acid (HA) from seawater and methyl orange (MO) dye from aqueous solutions. Phosphoric acid H_3PO_4 was used as an activating agent for the chemical activation of these agricultural wastes. The characterization of the activated carbon obtained using a scanning electron microscope (SEM), Fourier-transform infrared (FTIR) spectroscopy analysis, X-ray diffraction (XRD) and the Brunauer–Emmett–Teller (BET) method revealed that the activated carbon products exhibited high porosity and the formation of various functional groups. The effects of different parameters were examined using batch adsorption experiments, such as the adsorbent masses, pH, initial pollutant concentration and contact time. The results show that the performance increased with an increased adsorbent mass (up to 0.25 g/L) and decreased initial concentration of the adsorbent tested. On the other hand, this study clearly showed that the adsorption efficiency of the MO on the raw spent coffee grounds (SCGs) waste was around 43%, while no removal was observed for the humic acid. The experiments demonstrated that the activated carbon synthesized from the used coffee grounds (the efficiency was compared with commercial activated carbon (CAC) with a difference of 13%) was a promising alternative to commercially available adsorbents for the removal of humic acid from seawater. To understand and elucidate the adsorption mechanism, various isothermal and kinetic models were studied. The adsorption capacity was analyzed by fitting experimental data to these models. The experimental data for methyl orange dyes were analyzed using Langmuir and Freundlich isothermal models. The Freundlich isotherm model provided a superior fit to the equilibrium data, as indicated by a higher correlation coefficient (R^2) than that of the Langmuir model. The maximum adsorption was observed at pH 3. The Freundlich adsorption capacity was found to be 333 mg/g adsorbent. The PAC showed a high adsorption capacity for the MO and HA. The PAC showed the highest adsorption capacities for the HA and MO compared with the other adsorbents used (SCGs and CAC) and would be a good material to increase the adsorption efficiency for humic acid removal in the seawater pretreatment process. In addition, the prepared AC BET surface area was 520.40 m²/g, suggesting a high adsorption capacity. This makes the material potentially suitable for various applications that require a high surface area. These results indicate

that high-quality sustainable activated carbon can be efficiently produced from coffee waste, making it suitable for a wide range of adsorbent applications targeting various pollutants.

Keywords: spent coffee; activated carbon; adsorption; humic acid; methyl orange dye; chemical activation; seawater; kinetic

1. Introduction

Recently, due to rapid development, organic and inorganic waste has become a major threat to the natural environment and human health worldwide. However, poor waste management, including storage, poses significant environmental risks, leading to water and soil pollution [1–3]. The amount of waste and synthetic chemicals released into the environment is increasing daily [4–6]. The diversity of pollutants in water complicates the process of purifying different types of pollutants, which require different treatment methods. Among these pollutants are dyes that are widely used in various industrial processes, such as dyes, plastics, textiles, cosmetics, paper and food, which consume significant quantities of water in their production [7–10]. Similarly, synthetic dyes, such as methyl orange (MO), widely used in various industries, are another group of recalcitrant organic pollutants commonly found in industrial wastewater [11]. MO is known for its toxicity and potential carcinogenic effects and poses serious risks to aquatic life and human health when discharged into water bodies without adequate treatment [12,13]. Of the many techniques designed to remove dyes, adsorption is one of the most effective and has been used successfully to remove dyes from wastewater. Growing concerns about environmental pollution and the depletion of natural resources have prompted researchers to explore sustainable, cost-effective solutions for water treatment. Adsorption has become a highly effective and widely used method for removing organic contaminants from water [14–16]. The advantages of this technique include high efficiency, cost-effectiveness and the ability to treat large volumes of water [17–19]. In particular, activated carbon is widely used as an adsorbent due to its high surface area and porous structure, which facilitate the effective adsorption of a wide range of contaminants present in aqueous solutions [20–22].

The most promising approach is to convert and valorize organic waste into value-added products, such as activated carbon (AC). In recent years, there has been growing interest in the production of AC from agricultural and industrial waste [23,24]. These materials are often abundant and inexpensive, making them attractive raw materials for AC synthesis. What is more, converting waste into a useful product is in line with the principles of the circular economy [25,26]. A great deal of research has focused on the development of activated carbon from organic waste, offering a sustainable and environmentally friendly approach to water treatment. Alternatives aimed at reducing the quantity of waste or finding new applications for it are therefore being sought. Organic agricultural waste in particular has attracted attention as a promising raw material for the production of activated carbon. They are available in abundance and have demonstrated substantial adsorption capacity for a wide range of organic and inorganic pollutants, making them a viable option for water purification applications [27]. Recently, several review articles explored the potential of residue-based adsorbents for water and wastewater treatment, with applications mainly focused on the removal of micropollutants, such as heavy metals, dyes and pigments, pesticides, pharmaceuticals, other contaminants from industrial chemicals and even plastic residues, for environmental protection and sustainable development [28–30]. Numerous studies examined the effectiveness of activated carbon prepared by physical or chemical activation from various agricultural wastes in removing pollutants from dye-contaminated wastewater [21]. These wastes include date, olive and apricot pits [31,32]; corn cob residues [33]; rice husks and straw [34]; cocoa husks [35]; coconut husks [36]; lignin [37]; oil palm husks [38]; sunflower seed husks [39]; and jute sticks [40]. Numerous studies focused on the optimization of activated carbon (AC) prepa-

ration conditions, and used coffee grounds are attracting a great deal of interest due to their high consumption and wide availability. Due to its particular characteristics, this waste could represent a viable circular economic model for the large-scale production of activated carbon for commercial applications, such as seawater pretreatment processes, wastewater treatment and water purification [41–46]. Several researchers developed activated carbon from coffee waste for the adsorption of various organic pollutants, including dyes, such as methylene blue (MB), bromothymol blue (BB) and acid orange 7 (AO7), as well as toxic inorganic pollutants, such as fluoride and phenol; the antibiotic lomefloxacin; and heavy metals, such as iron (Fe), orthophosphate, lead (Pb(II)) and cadmium (Cd(III)) [47–50]. Among the various approaches to removing dyes from aqueous solutions, adsorption on activated carbon is one of the most effective and widely used techniques [48,51–53]. Jung, K et al. [53] investigated a cost-effective method for removing methylene blue (MB) and acid orange 7 (AO7) dyes from aqueous solutions using activated carbon derived from SCGs. The activated carbon was incorporated into porous calcium alginate beads to enhance its performance. The results revealed that the adsorption efficiency was highly dependent on the solution pH, which influenced the binding affinity between activated carbon and dye molecules. However, the process was not affected by ionic effects. In addition, the study indicates that the surface of activated carbon is energetically heterogeneous and that the adsorption process follows an endothermic mechanism. Egle Rosson et al. [54] evaluated the removal efficiency of phenol, chlorophenol and bisphenol-A by adsorption using powdered activated carbon from used coffee grounds. Their results showed that the removal efficiency was linked to the highest partition coefficients for methylene blue and 3-chloropheno. On the other hand, the lower adsorption efficiency of bromothymol blue and bisphenol-A was due to their different surface properties. The same results were obtained by Popovici et al. [55] for the removal of phenol from aqueous solutions. For the removal efficiency of total iron and orthophosphate (PO₄-P), [53] Ching et al. [42] studied the effect of the impregnation ratio (IR) of sulfuric acid on the physical properties of prepared activated carbon. A high pore surface area and micropore volume were obtained with IR = 2.5 and 0.5 for the adsorptions of total iron and PO₄-P, respectively.

This abundant literature shows that activated carbon derived from used coffee grounds is capable of removing many pollutants from aqueous solutions, whereas the removal of humic acid from seawater has not yet been studied to our knowledge. However, very few studies examined MO removal using activated carbon derived from SCGs as the best adsorbent. In this context, the present work focused on the preparation and characterization of activated carbon derived from spent coffee grounds (SCGs) waste as a cost-effective adsorbent and its application to evaluate the efficiency of methyl orange (MO) removal from aqueous solutions and humic acid from Mediterranean seawater through an experimental batch adsorption process. The adsorbents used were also characterized using SEM, FTIR and XDR. Several operational parameters, including the adsorbent mass, pH, initial adsorbate concentration (pollutants) and contact time, which influenced the adsorption process, were analyzed using kinetic adsorption isotherms. In addition, experiments were carried out to assess the feasibility and performance of activated carbon (PAC) prepared with phosphoric acid H₃PO₄ and thermally activated at 550 °C. Depending on the waste treatment method, SCG upgrading led to material products that enabled the virtually complete removal of pollutants from water under optimal conditions. This work aimed to provide more in-depth information on the adsorption of humic acid (HA) in salt water, offering valuable insights for future work.

2. Materials and Methods

The chemicals used in this work were of analytical reagent grade. Methyl orange and phosphoric acid were obtained from Sigma-Aldrich (Merck KGaA, Darmstadt, Germany), with the methyl orange having a purity of 85%, while the humic acid had a purity of 60–70% (Table 1). Pure water obtained from a Millipore Milli-Q Academic ultra-pure water purification system was used for preparing all the solutions. A Quanta 250 Scanning

Electron Microscope (SEM) from Thermo Fisher Scientific (TFS), Waltham, MA, USA, with a tungsten filament was used to examine the microscopic morphology of the materials. X-ray Diffraction (XRD) measurements were performed using a BRUKER D8 Advance A25 focus diffractometer from Bruker Corporation, Billerica, MA, USA, within a 2-theta angle range of 20° to 80°. Fourier-transform infrared (FTIR) spectroscopy was performed on a BRUKER spectrophotometer (500–4000 cm⁻¹ range) from Bruker Corporation, Billerica, MA, USA, for the determination of various functional groups. The effect of absorbance and concentration on the pollutant adsorption in the aqueous solution was evaluated using UV–visible spectrophotometry (SHIMADZU UV-1800) from Shimadzu Corporation, Kyoto, Japan. Thermal activation of the materials was performed in a muffle furnace “Nabertherm”, heated at a rate of 10 °C/min from 50 °C to 550 °C. The specific surface area of the activated carbon was measured using nitrogen adsorption isotherm data at 77.35 K by utilizing the Brunauer–Emmett–Teller (BET) method using an Automated ASiQwin (Autosorb iQ) from Quantachrome Instruments, Boynton Beach, FL, USA.

Table 1. Characteristics of MO and HA.

Property	Value	
IUPAC name (*)	Sodium-4-(4-dimethylamino phenyl diazenyl) benzenesulfonate	Humic acid Na salts
Molecular formula	C ₁₄ H ₁₄ N ₃ NaO ₃ S	C ₉ H ₈ Na ₂ O ₄
Molecular weight (g/mol)	327.34	226.14
pKa	3.4	3–5
λ _{max} (nm)	464	254
Purity %	85	60–70
Color and form	Orange-yellow powder or crystalline scales	Dark brown to black powder
Melting point (°C)	>300	300
Solubility	Less than 1 mg/mL at 18 °C	

* IUPAC: International Union of Pure and Applied Chemistry.

In the experimental procedure, the experiments were conducted in triplicate to ensure the high precision and reliability of the results. Sometimes several tests were repeated to verify the reproducibility and confirm that the results were within an acceptable range (usually below 5%).

2.1. Preparation of Synthetic Solutions (Sorbate)

In this study, two synthetic solutions were prepared to evaluate the adsorption efficiency of the engineered activated carbon, which contributed to its optimization in water treatment processes for the removal of simple dyes and complex organic compounds. The first synthetic solution was prepared with methyl orange (MO), an anionic organic azo dye obtained from Sigma-Aldrich (USA) (CAS No. 547-58-0). This dye was chosen for its analytical quality with 100% purity, which guaranteed accurate and reliable results in the adsorption tests. It is characterized by the presence of an azo group (-N=N-) linking two aromatic rings, one of which contains a sulfonic acid group (-SO₃H), which increases its solubility in water and enhances its reactivity. The color of MO changes from red under acidic conditions to yellow under alkaline conditions.

The second solution was prepared with humic acid (HA), which is a complex structure comprising various functional groups, from Biochem Chemopharma (CAS no. 1415-93-6). It is partially soluble in water and more soluble in alkaline solutions, making it useful in a variety of applications. The chemical structures and properties are presented in Figure 1 and Table 1.

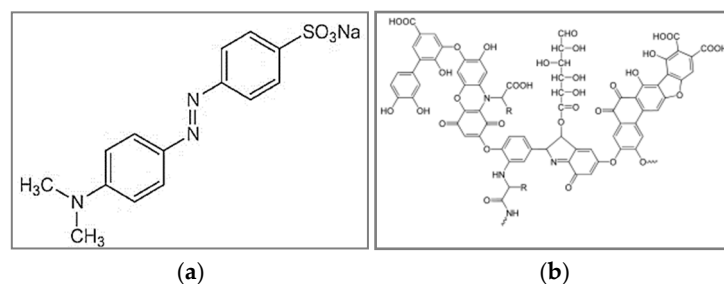


Figure 1. Chemical structures, (a) methyl orange (MO) and (b) humic acid (HA).

Stock solutions were prepared by dissolving 1 g MO in 1 L pure water, while 1 g humic acid was added to 62.5 mL NaOH (2N) solution due to its complex nature, then made up to 1 L with pure water and placed under continuous magnetic stirring for 24 h [56]. NaOH helps dissolve humic acid by neutralizing the acidic functional groups, forming a more soluble salt. Test solutions were prepared by diluting the MO or HA stock solution with pure water to obtain the appropriate concentration of the desired solutions. Four test solutions of different C_0 concentrations, namely, 5, 10, 20 and 40 ppm, were prepared and completed by dilution. Absorbance calibration curves were plotted against the concentration of each pollutant used.

The degradation of methyl orange (MO) and humic acid (HA) was assessed by measuring the absorbance using a UV–visible spectrophotometer (Shimadzu UV-1800). The maximum absorption wavelengths were identified at 464 nm for MO and 264 nm for HA. A correlation curve that related the concentrations of MO and HA to their respective absorbance was established prior to the measurements. The absorbance response showed excellent linearity over the concentration range of 2–100 ppm, with a high correlation coefficient of 0.99. This strong linear relationship confirmed the reliability and precision of the measurements within this concentration range, which ensured accurate quantification in our adsorption studies. The equations and relative standard deviation (R^2) were $y = 0.091x$ for the MO, with $R^2 = 0.999$, and $y = 0.003x$ for the HA, with $R^2 = 0.995$, where $R^2 = 0.995$ indicates an excellent fit and consistency.

The pH of each solution tested was adjusted to the required value with 0.1 M NaOH or 0.1 M HCl immediately prior to the sorbent application. The solutions were subjected to adsorption experiments to assess the effectiveness of the elaborated activated carbon in removing the methyl orange and humic acid from the aqueous solutions. For the experiments, we used seawater collected near Fouka beach, Wilaya de Tipaza, and its physical and chemical properties are presented in Table 2. Seawater is particularly contaminated with humic acid, making its removal crucial during the seawater pretreatment phase of reverse osmosis desalination to ensure the efficiency of subsequent treatment processes. To address this, in a real seawater pretreatment application, CA prepared from used coffee grounds was used and tested to maximize the removal of trace organic and inorganic substances, including humic acid, through adsorption [57].

Table 2. Results of physico-chemical analyses of Fouka Seawater, Tipaza, Algeria.

Parameters	Value	Parameters	Value
Conductivity (mS/cm)	56.2	Bicarbonates HCO_3^- (ppm)	134
Salinity	35.8	TH	450.3
pH	7.7	Calcium Ca^{2+} (ppm)	220
Turbidity (NTU)	1.05	Magnesium mg^{2+} (ppm)	807
TDS (g/L)	36.1	Chlorides Cl^- (ppm)	6532
MES (ppm)	4.6	Potassium K^+ (ppm)	145.7
Nitrite NO_2^- (ppm)	5.8	Fe^{2+} (ppm)	0.09
TAC	13.4	Sulfate SO_4^{2-} (ppm)	1100

The complex structure of humic acid molecules can lead to membrane clogging and increased resistance to feed flow, highlighting the need for effective removal techniques. Below, we demonstrate the effectiveness of the Bou-Ismaïl seawater pretreatment process in removing pollutants by evaluating the adsorption capacities of activated carbon developed at different concentrations. The adsorption efficiency was tested using Bou-Ismaïl seawater from Tipaza, Algeria, characterized by a salinity of 35 g/L and an electrical conductivity of 58 mS/cm (Table 2), which was enriched with humic acid at concentrations of 5, 10, 20 and 40 ppm.

2.2. Preparation of Activated Carbon (Adsorbent)

In our case, used coffee grounds, a common organic waste, were chosen for their reuse and recovery potential as a precursor for activated carbon production due to their abundance and carbon-rich composition. This raw material was collected from various cafeterias in the city of Algiers, Algeria. They were cleaned several times with hot water, air-dried for a week and then sieved. The first step in the process of obtaining carbon adsorbents was chemical activation using SIGMA-ALDRICH's phosphoric acid (H_3PO_4). Then, the impregnation ratio defined by the weight ratio of H_3PO_4 to coffee grounds was used to control and ensure optimal activation. This process developed a porous structure, which improved the adsorption capacity of the final activated carbon. Chemical activation was carried out by impregnating used coffee grounds with 1:1 H_3PO_4 for 24 h, followed by drying at 100 °C for 24 h. After chemical activation, the product was washed and filtered several times with pure water, then dried in an oven at 110 °C for 24 h. The H_3PO_4 -activated materials were subjected to carbonization by heating in a high-temperature oven at 550 °C (pyrolysis) [57].

During carbonization, organic matter undergoes pyrolysis, resulting in the formation of carbon. This material has an increased porosity and surface area, making it suitable for adsorption applications. In addition, for a possible comparison with activated carbons produced from used coffee grounds, the adsorption efficiency of a commercial AC (CAC) and raw used coffee grounds (SCGs) was carried out. The adsorption experiments were carried out in 250 mL beakers under constant magnetic stirring (350 rpm) at room temperature in batch mode. The adsorption study was carried out in a natural solution without pH adjustment. Each beaker that contained the initial sorbent concentration C_0 of MO and HA and the adsorbent weights of AC, CAC and SCG was used separately. For a given time, the samples were filtered and analyzed by a "SHIMADZU UV-1800" UV-vis spectrophotometer with UV absorption detection (Table 1). For the adsorption kinetics, the effect of the initial concentration C_0 , contact time (5–120 min) and sorbent weight were evaluated. The $E\%$ efficiency of the adsorption process indicates the percentage of the initial pollutant adsorbed by the adsorbent material. It was calculated from Equation (1). In addition, the adsorption capacity Q_t (mg/g) at time t reflects the amount of pollutant adsorbed per unit mass of adsorbent. The adsorbed quantity Q_t (mg/g) was calculated as shown in Equation (2) using the difference between the initial pollutant concentration in solution C_0 (ppm) and the final concentration C_t (ppm).

$$E\% = \frac{(C_0 - C_t)}{C_0} \times 100 \quad (1)$$

$$Q_t = \frac{(C_0 - C_t) \cdot V}{m} \quad (2)$$

where C_t is the concentration of the pollutant in the solution (ppm) at time t , V is the volume (L) of the solution and m is the mass of the adsorbent (g) AC.

Adsorption isotherms are essential tools for understanding the interactions between an adsorbate and an adsorbent. They describe how the amount of adsorbate on the surface of the adsorbent changes as a function of its concentration in solution at a constant temperature. Several models were developed to analyze the adsorption equilibrium data, with each providing information on different aspects of the adsorption process.

The linear forms of the Freundlich and Langmir isotherms equations are given by

$$\ln Q_e = \ln K_f + \frac{1}{n} \ln C_e \quad (3)$$

$$\frac{1}{Q_e} = \frac{1}{Q_m} + \left(\frac{1}{K_L} Q_m \right) \cdot \frac{1}{C_e} \quad (4)$$

where Q_e is the amount of adsorbate adsorbed per unit mass of adsorbent at equilibrium (mg/g); C_e is the equilibrium concentration of the adsorbate in the solution (ppm); K_f is the Freundlich adsorption constant (indicating the adsorption capacity); n is the Freundlich constant related to the adsorption intensity; Q_m is the maximum adsorption capacity (mg/g), representing the saturation capacity of the adsorbent; and K_L is the Langmuir constant related to the adsorption energy (L/mg).

3. Results and Discussion

3.1. Characterization of Adsorbent

To characterize the morphology of the activated carbon produced from used coffee grounds, an analysis was carried out with a scanning electron microscope (SEM) at different magnifications (50, 30 and 10 μm) to examine the surface structures and structural changes between the raw coffee grounds and prepared activated carbon. Figure 2 shows a rough surface with narrow cavities, which is characteristic of lignocellulosic materials.

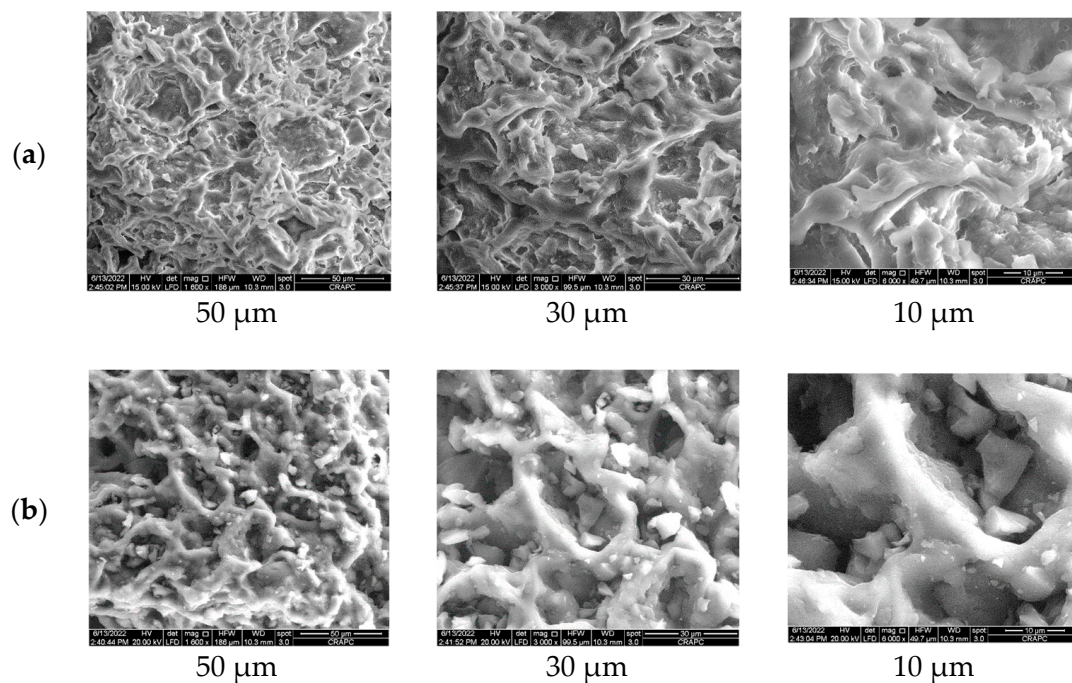


Figure 2. SEM images of materials taken at different magnifications before and after chemical activation with H_3PO_4 and pyrolysis at $550\text{ }^\circ\text{C}$, (a) Spent coffee grounds (SCGs) before chemical activation and (b) Prepared activated carbon from SCGs (after chemical activation).

This observation suggests that the original structure of the precursor material, namely, coffee grounds, was largely preserved, even after the pyrolysis process (Figure 2a,b). The cavities observed contributed to the porous structure required for efficient adsorption and suggest that the carbonization process increased the surface area of the material without completely altering its original morphology. The outer surface of the activated carbon features uniformly distributed the cavities that were formed during the activation process by the chemical additive H_3PO_4 , which created a porous structure, and through carbonization, freed up occupied space and increased the specific surface area. These

results led us to select the prepared ACs for adsorption optimization tests of the HA complex organic substances and MO dyes. The difference between the FTIR spectra of the SCGs before and after the chemical activation with the H_3OP_4 is shown in Figure 2. The broad band observed between 3000 cm^{-1} and 3500 cm^{-1} corresponded to the stretching vibrations of OH hydroxyl groups, which were associated with both the coffee grounds and water structures. Typically, a broad peak around 3219.57 cm^{-1} is attributed to the vibration of hydrogen-bonded OH groups. However, in the activated carbon sample, this peak was completely absent, indicating the removal of OH groups during the activation process [57].

The elemental content of activated carbon, particularly carbon (C); oxygen (O); and other elements, such as hydrogen (H), nitrogen (N) and sulfur (S), can vary depending on the source of the biomass, the activation process and the treatment conditions. The elemental composition of activated carbon is predominantly carbon (70–90%), with oxygen (5–20%) and small amounts of hydrogen, nitrogen and sulfur. The precise composition depends on the raw material, activation method and temperature, and it plays a crucial role in the adsorption capacity and surface characteristics of the material. The BET analysis indicated a calculated specific surface area of $520.40\text{ m}^2/\text{g}$, suggesting a significant adsorption capacity. This makes the material potentially suitable for various applications that require a high surface area.

Figure 3a shows a broad band from 2900 cm^{-1} to 2700 cm^{-1} associated with elongation and the presence of the C-H group in the SCG raw material. After activation, this C-H group was eliminated, indicating the removal of aliphatic hydrocarbon chains during the activation process. Two peaks at 2919.57 cm^{-1} and 2852.01 cm^{-1} that corresponded to the formation of the CH_2 group in SCGs, associated with C-H bond elongation, were observed. In addition, two peaks of average intensity at 1644.40 cm^{-1} and 1536.76 cm^{-1} were observed that corresponded to the C=C bond, which is typical of alkenes or aromatic structures in SCGs. Figure 3b shows the appearance of two peaks between 2000 cm^{-1} and 2500 cm^{-1} , which were probably related to the C=C stretching vibrations of alkenes and aromatic compounds. In the $2000\text{--}2500\text{ cm}^{-1}$ range, two peaks were observed at 2185.84 cm^{-1} and 1985.75 cm^{-1} , which were related to the $\text{C}\equiv\text{C}$ stretching vibrations of the carbon-carbon triple bond in alkynes. A peak was observed at 1558.43 cm^{-1} that corresponded to C-H deformation (bending) vibrations. The peak observed at 1159.06 cm^{-1} typically corresponds to stretching vibrations of phosphate groups. The two peaks with average intensities of 474.60 and 402.28 cm^{-1} corresponded to the phosphoric element.

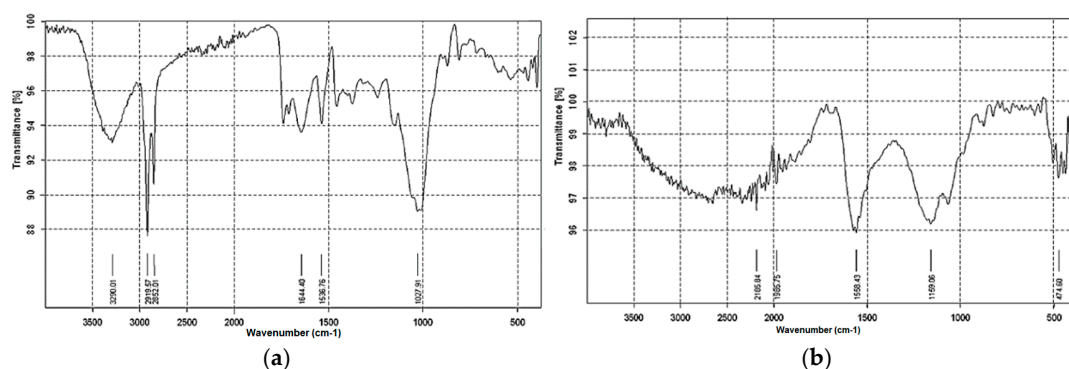


Figure 3. Fourier-transform infrared (FTIR) spectra of materials: (a) raw spent coffee grounds and (b) prepared activated carbon.

The crystal structure and phase purity of the materials used, such as the SCGs and PAC, were examined by X-ray diffraction (XRD), which can provide valuable information on their structural characteristics. The XRD patterns of the materials before and after the activation are shown in Figure 4, with both the XRD patterns showing an amorphous structure. The XRD pattern of the used coffee grounds showed a broad diffraction peak at $2\theta = 19.77^\circ$ and an intensity of $I = 4993$, which was attributed to the amorphous or poorly ordered organic components in the SCGs (cellulose, lignin organic materials). A small peak at

35.32° ($I = 2081$) was attributed to the presence of crystalline components and may indicate traces of inorganic phases or other mineral residues present in the SCGs. In addition, the XRD pattern of the activated carbon showed a broad peak around $2\theta = 25.74^\circ$ ($I = 4455$), which was associated with the amorphous carbon structure and signified a disordered arrangement of carbon atoms with some degree of graphitic character. When comparing the intensity values of X-ray diffraction (XRD) analysis between the PAC and SCGs, we observed that the intensity of the PAC started at 5458, while that of the SCGs started at 3079. This suggests that the PAC had more pronounced or concentrated crystalline features than the SCGs [57].

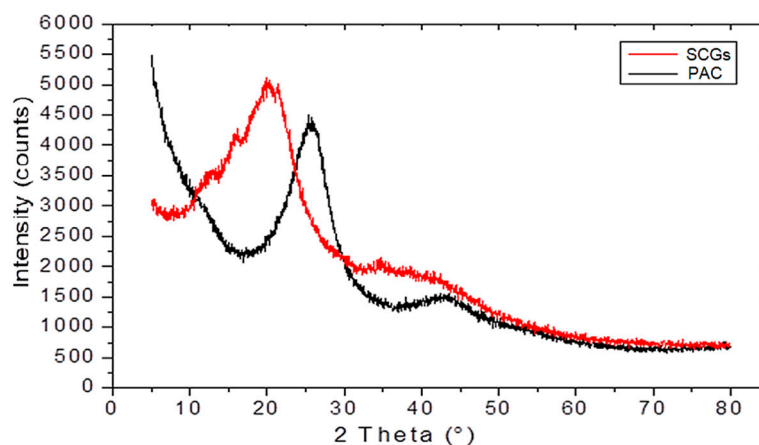


Figure 4. X-ray diffraction (XRD) of materials used: SCGs and PAC.

3.2. Adsorption Isotherms

Effects of Different Parameters on the MO Adsorption Process

The effect of different factors on the MO and HA removal by the SCGs, PAC and CAC, such as pH, adsorbent mass (weight), initial pollutant concentrations and contact time, was examined.

We examined the effect of the initial pH of the MO solution on the adsorption for an initial concentration of 10 ppm at different pH values (3, 5, 7 and 9) using a PAC adsorbent mass of 0.25 at room temperature $T = 22^\circ\text{C}$ for 120 min. A significant change in the amount adsorbed by the PAC for the pH values studied was noted (Figure 5). An efficiency ($E\%$) of 52% for the MO removal was recorded in 5 min at $\text{pH} = 3$, which then increased to reach an optimal value of 96% in 60 min, finally reaching 100% for a contact time of 90 min. On the other hand, for pH values above 5, we observed decreases in the relatively low adsorption rates of 94%, 98.6% and 100% for pH 5, 7 and 9, respectively. We found that when the pH was above pH_{pzc} (5.2), the activated carbon surface was positively charged, while the anionic MO dye molecule in the solution was negatively charged. The adsorption resulted from the electrostatic interactions between the charged activated carbon and the MO dye. As the pH decreased, these interactions intensified, where the activated carbon surface became more positively charged and the solution more acidic. Table 3 summarizes the resulting data on the zeta potentials and surface charges at different pH values.

As shown in Table 3, the zeta potential of the activated carbon varied significantly with the pH, which influenced the surface charge. At low pH (acidic conditions, pH 2), the surface of activated carbon becomes protonated, resulting in a positive zeta potential. This positively charged surface enhances the adsorption of negatively charged species, such as humic acid and methyl orange. In contrast, at high pH, the surface becomes deprotonated, leading to a negative zeta potential. This negative charge can reduce the adsorption efficiency of anionic substances due to electrostatic repulsion between the similarly charged surface and the adsorbates.

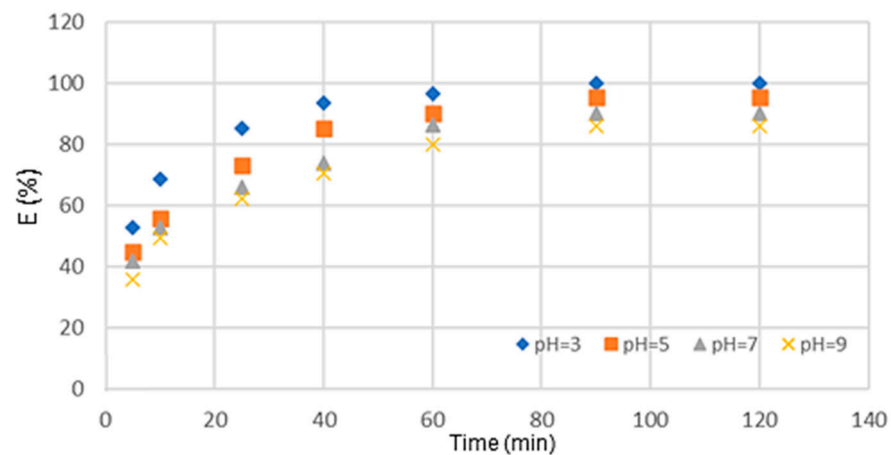


Figure 5. Effect of initial pH on MO removal yield ($C_0 = 10$ ppm, $m = 0.25$ g/L, $T = 24$ °C).

Table 3. Effect of pH on zeta potential and surface charge of activated carbon.

pH	Zeta Potential (mV)	Surface Charge
2	+30 to +40 mV	Strong positive charge
4	+10 to +20 mV	Moderate positive charge
6	+5 to 0 mV	Weak positive charge/neutral
8	−5 to −15 mV	Weak negative charge
10	−20 to −30 mV	Moderate negative charge
12	−40 to −50 mV	Strong negative charge

The effect of the adsorbent mass on the MO dye removal by the PAC was studied for different adsorbent weights (0.01, 0.05, 0.125, 0.25 g), as shown in Figure 6. The curves representing the variation in the removal rate (E%) show an increase over time for the different adsorbent weights. The adsorption kinetics results indicate that with a low CAP mass of 0.01 g, the removal efficiency increased from 16% (5 min) to 60% (60 min). It was noted that with an adsorbent mass of 0.25 g, the MO adsorption efficiency increased significantly, from 50% at 5 min to 86% at 60 min, indicating that the amount of adsorbent was attributed to the increase in the number of active sites. The maximum efficiency was achieved with adsorbent masses of 0.01 g and 0.25 g, which reached 61% and 90% at 120 min, respectively. An adsorbent mass of 0.25 g appeared to be optimal for the MO removal experiments by the PAC.

The effect of the initial MO dye concentration was realized by increasing its concentration from 5 to 40 ppm. For the initial concentration $C_0 = 5$ ppm, the adsorption removal efficiency increased from 72% (5 min) to 100% (60 min), as shown in Figure 7. We note that increasing the concentration of the MO dye in the solution from 5 to 40 ppm resulted in a decrease in the adsorption efficiency from 100% to 70%. This indicates the progressive saturation of the PAC adsorption sites for a given quantity. These experimental results show that the MO adsorption by the PAC was dependent on the initial concentration. Comparable patterns were observed in previous studies using activated carbon derived from organic waste for dye removal.

Figure 8 shows the comparison of the adsorption kinetics in terms of the evolution of the adsorption efficiency (E%) as a function of time for the different adsorbents considered, namely, the SCGs, CAC and PAC. The MO removal rates increased with the contact time for the CAC and PAC sorbents, which reached saturation in 60 min. On the other hand, the adsorption on the SCGs increased within 10 min, then stabilized at around 43% efficiency. We can see that the rate of the MO removal by the used coffee grounds was much lower—a

difference of 52%—than that recorded with the PAC at 60 min. In this work, we note that the efficiency of the PAC we developed exceeded that of the commercial CAC by around 13%.

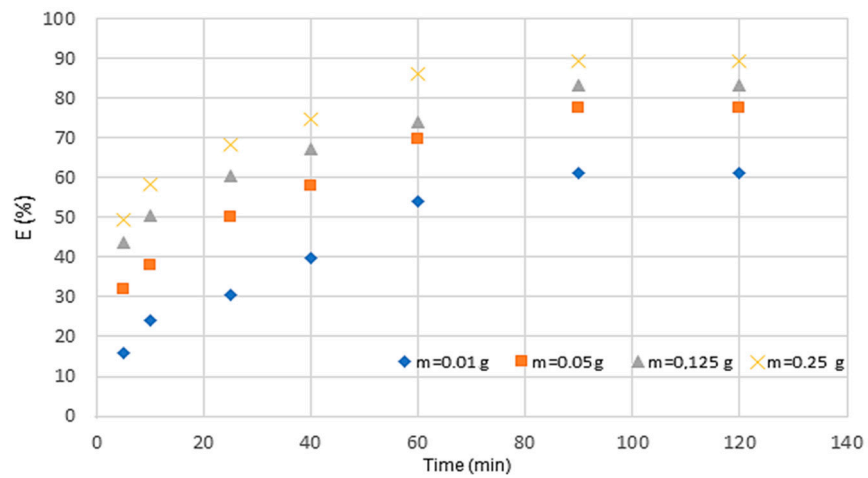


Figure 6. Effect of the adsorbent mass of the PAC on the MO elimination rate ($C_0 = 10$ ppm, $T = 24$ °C).

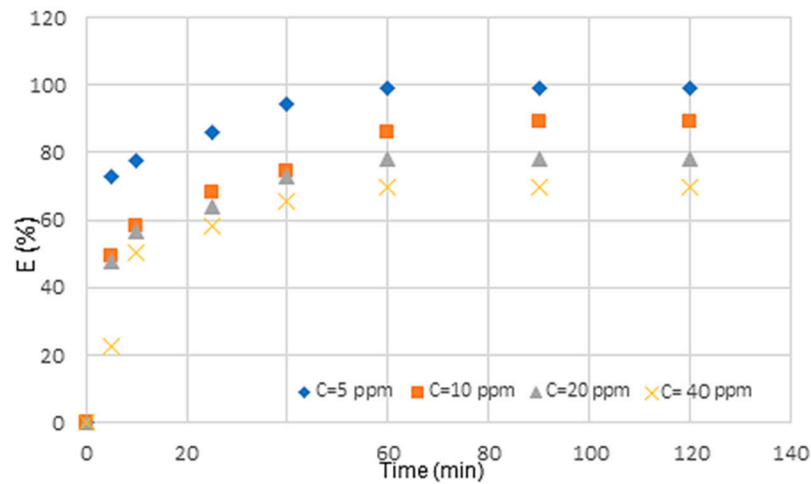


Figure 7. Effect of initial MO dye concentration on efficiency E% of MO removal ($m_{PAC} = 0.25$ g, $t = 5$ –120 min, $T = 24$ °C).

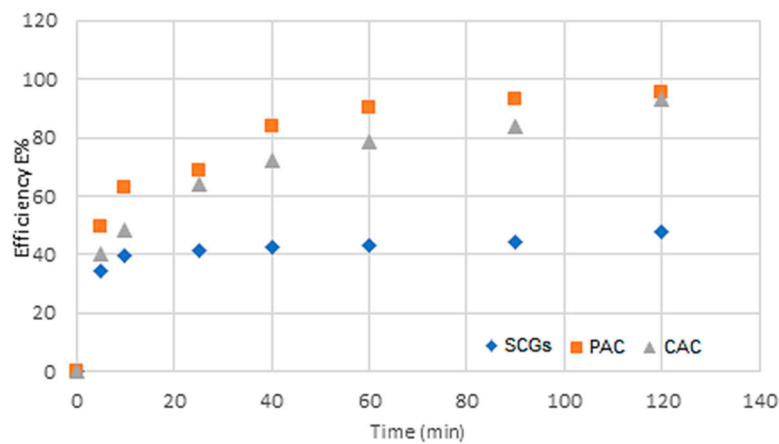


Figure 8. Evolution of the adsorption efficiency of the MO as a function of time for the different adsorbents: SCGs, CAC and PAC ($C_0 = 10$ ppm, $m = 0.25$ g, $T = 19$ °C).

Figure 9 shows the adsorption isotherm for the MO on the PAC, describing and illustrating the interaction (adsorbent/adsorbent) between the amount of the MO dye adsorbed and its equilibrium concentration in the solution. The adsorption capacity increased progressively with the initial MO concentration. The resulting isotherm curve resembled an L-type isotherm, indicating strong adsorption properties between the adsorbent and adsorbate at low concentrations. However, as the MO concentration increased, the adsorption capacity decreased due to the progressive saturation of the adsorbent material. The parameters of the MO adsorption isotherms and those of the pseudo-first- and second-order model kinetics were calculated and are presented in Tables 4 and 5. From Table 4, we obtained a maximum adsorption capacity of 333 mg/g for the Freundlich model, with an R^2 value of 0.944. Furthermore, we found that the equilibrium adsorption quantity Q_t in both the pseudo-first-order (PFO) and second-order (PSO) models increased with the initial concentration, while the rate constant Kv decreased, as shown in Table 5, where Kv is an indicator of the adsorption capacity of the MO. Furthermore, we observed that the R^2 values for the PSO model were higher than those calculated using the PFO model. Therefore, we suggest that the PSO model was more appropriate to describe the adsorption kinetics of the MO on the PAC [57].

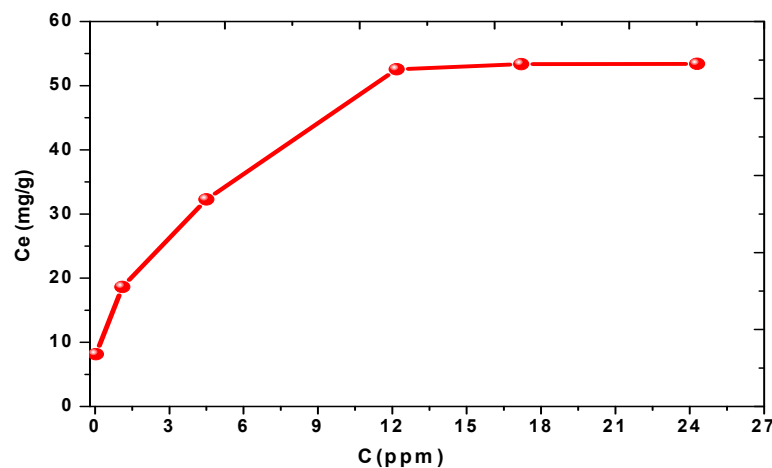


Figure 9. Adsorption isotherm curve for MO on prepared activated carbon.

Table 4. Langmuir and Freundlich isotherm constants in case of MO.

Langmuir Model			Freundlich Model		
K_l (L mg ⁻¹)	Q_{max} (mg g ⁻¹)	R^2	K_f (L mg ⁻¹)	n	R^2
0.096	333.33	0.904	26.76	3.05	0.944

Table 5. Kinetic parameters of the pseudo-first- and second-order models.

MO Dye		PFO		PSO		
C_0 (ppm)	Kv (min ⁻¹)	Q_e (mg g ⁻¹)	R^2	Kv (min ⁻¹)	Q_e (mg g ⁻¹)	R^2
5	0.063	4.85	0.873	0.052	8.84	0.999
10	0.046	13.58	0.933	0.0097	19.60	0.995
20	0.065	22.80	0.931	0.0092	33.33	0.998
40	0.045	37.07	0.850	0.0030	62.5	0.994

Table 6 provides a comparative analysis of the different agricultural waste materials used for the removal of methyl orange (MO) dye. Additionally, it emphasizes the importance of utilizing waste as a sustainable source for new products and applications. This analysis highlights the effectiveness of these adsorbents, offering key insights into

their potential for cost-effective and environmentally friendly water treatment solutions. Notably, the adsorption efficiency and isotherm models are significantly influenced by the type of raw material used. In our case study, the comparison revealed that the MO dye was removed with the highest adsorption efficiency.

Table 6. Comparative study of activated carbon derived from various waste sources for methyl orange dye removal.

Agricultural Waste Materials as Sources of AC	Fitted Isotherm Model	Fitted Kinetic Model	Efficiency (%)	Reference
Date Stones	Freundlich isotherm	Pseudo-second-order	76.6	[58]
Prickly Pear Seed Cake	Freundlich isotherm	Pseudo-second-order	-	[59]
Waste tire rubber	Langmuir isotherm	Pseudo-second-order	80	[60]
Popcorn	-	Pseudo-second-order	48.5	[61]
Coffee grounds	Freundlich isotherm	-	60–65	[62]
Spent coffee grounds	Freundlich model	Pseudo-second-order	99.01	Present study

3.3. Adsorbent for Seawater Pretreatment Application

Humic Acid Removal from Seawater

Figure 10 shows the effect of the PAC adsorbent mass and solution pH on the humic acid removal efficiency for the concentration $C_0 = 10$ ppm. The HA removal rate from the seawater reached its maximum value (60%) at $m = 0.25$ g, as shown in Figure 10a. As the adsorbent mass increased, the HA removal rate rose from 22.22% to 60%, demonstrating the complexity of the structure of humic acid molecules. The most efficient adsorption process was demonstrated at pH 3, as shown in Figure 10b.

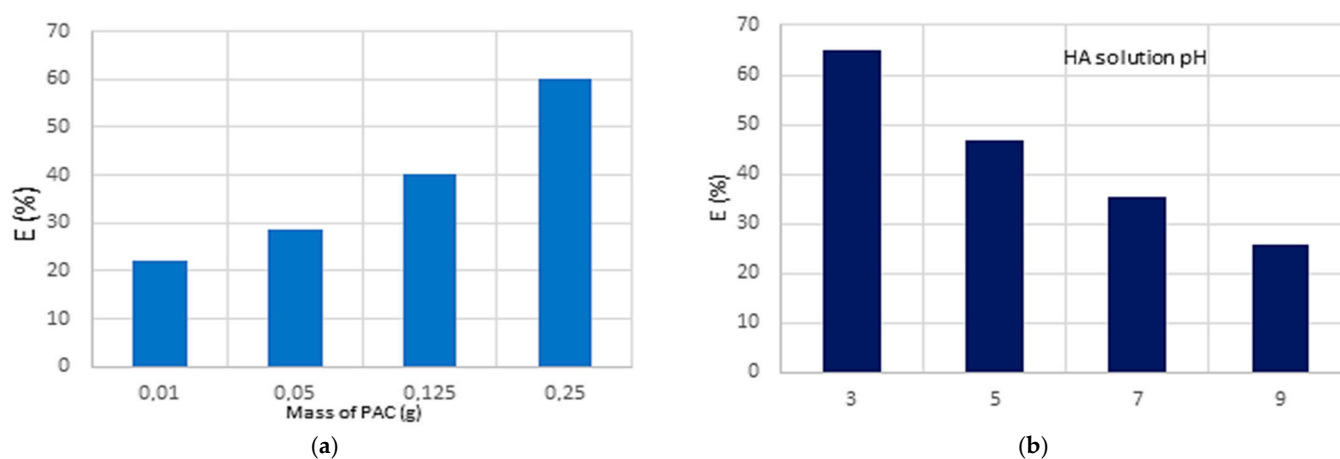


Figure 10. Effect of CAP carbon mass (a) and (b) solution pH on HA acid removal rate ($C_0 = 10$ ppm, $t = 90$ min).

Figure 11 shows the effects of the SCGs, CAC and PAC on the rate of the HA removal by adsorption as a function of time (120 min contact time). In this case, there was a big difference between the results obtained, where the raw coffee grounds had no effect on this elimination process. Thus, the SCGs absorbed practically no humic acid, which may be explained by the complexity of the organic substance HA. However, we observed that the commercial PAC and CAC show promising capabilities for humic acid removal, with their performances being quite similar during the initial contact times $t < 10$ min. Our developed carbon, however, outperformed the commercial CAC for contact times above $t > 25$ min. For short contact times, the removal rate reached over 20% at $t = 5$ min and 35% at $t = 25$ min. This efficiency increased with time, exceeding 50% at $t = 60$ min, and the best $E = 60\%$ results

were obtained for a contact time of $t = 90$ min. The activated carbon produced showed good adsorption affinity with the humic acid, a highly complex element characterized by the highest humus fractions. The resulting isotherm models and kinetic parameters obtained are summarized in Tables 7 and 8. The kinetic adsorption models applied to describe the experimental data by non-linear regression include the pseudo-first-order and pseudo-second-order models are presented in Figures 12 and 13 for HA adsorption into PAC. The analysis indicates that the pseudo-second-order model provides the best fit for the adsorption of HA, with a high correlation coefficient ($R^2 = 0.999$) as shown in Figure 13. The adsorption behavior of activated carbon can be explained by several mechanisms. Physical adsorption through Van der Waals forces is significant due to the high surface area and porous structure of the carbon. In addition, chemical adsorption can occur via functional groups on the carbon surface, particularly for compounds like humic acid that can form hydrogen bonds or undergo ion exchange. Electrostatic interactions, influenced by pH, and π - π interactions between the aromatic rings of methyl orange and the carbon structure, further contribute to the adsorption process.

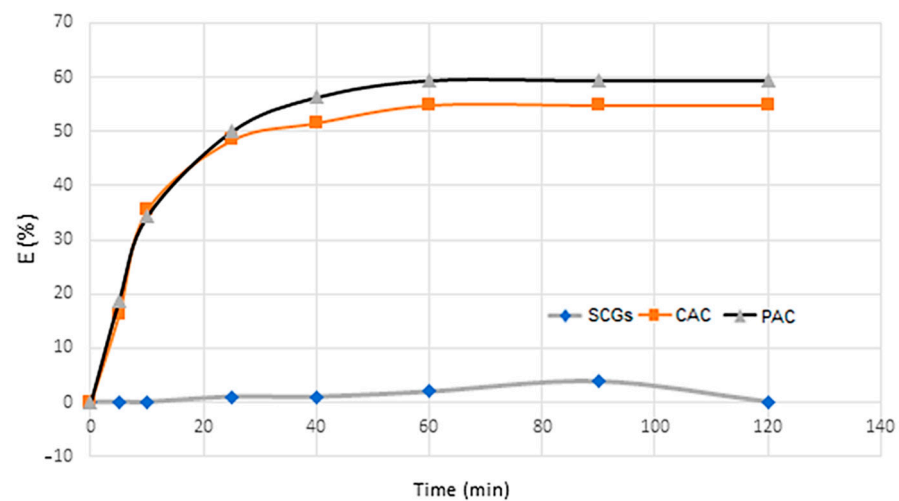


Figure 11. Evolution of humic acid adsorption yield versus time for different adsorbents: SCGs, CAC and PAC ($C_0 = 10$ ppm, $m = 0.25$ g, $T = 20$ °C).

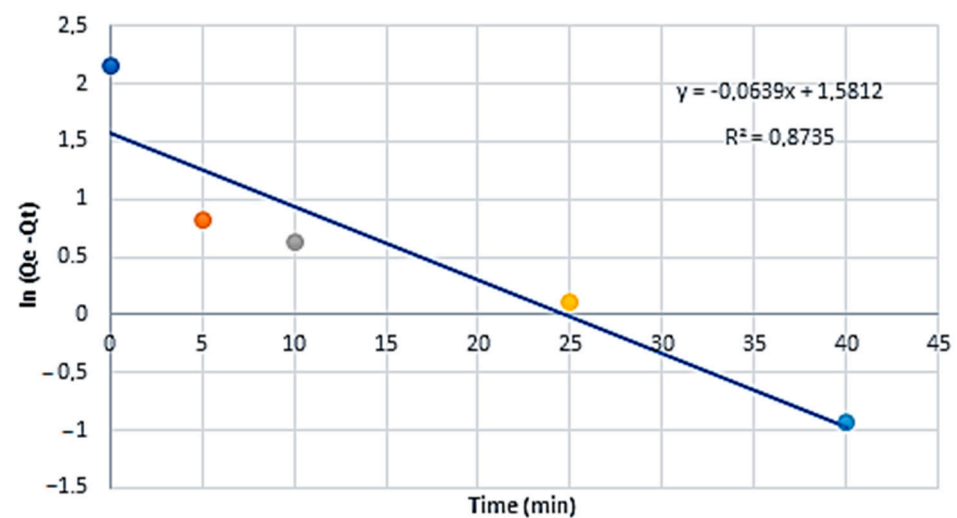


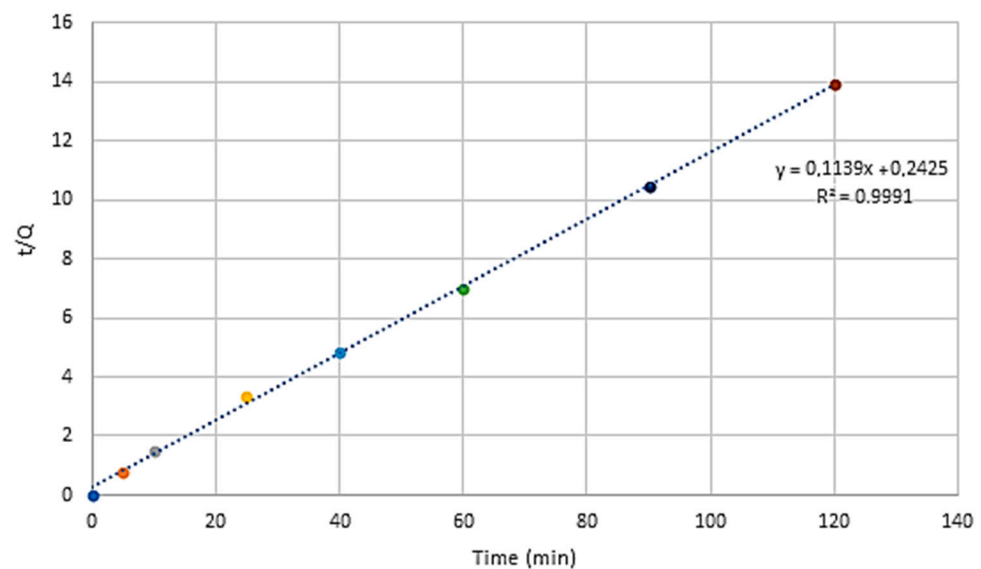
Figure 12. Pseudo-first-order kinetic variation for the HA for the adsorption by the PAC.

Table 7. Isotherm models used for the adsorption of the HA by the PAC.

Langmuir Model			Freundlich Model		
K (L mg ⁻¹)	Q_{max} (mg g ⁻¹)	R^2	K	n	R^2
0.789	3.134	0.178	6.800	4.016	0.916

Table 8. Kinetic parameters and correlation coefficients for the removal of the HA.

Humic Acid		PFO		PSO		
C_0 (ppm)	K_1 (min ⁻¹)	Q_e (mg g ⁻¹)	R^2	K_2 (min ⁻¹)	Q_e (mg g ⁻¹)	R^2
5	0.038	6.13	0.974	0.017	7.87	0.990
10	0.071	9.99	0.972	0.014	12.04	0.992
20	0.019	11.43	0.516	0.0016	17.54	0.795
40	0.034	17.32	0.972	0.0016	21.27	0.892

**Figure 13.** Pseudo-second-order kinetic variation for the adsorption of the HA by the PAC.

4. Conclusions

Adsorption is widely regarded as one of the most effective techniques for treating water contaminated with organic substances and dyes due to its simplicity, high efficiency and cost-effectiveness. Humic acids (HAs), which are complex organic compounds commonly present in seawater, brackish water and surface water, must be removed for effective water treatment. The development of novel adsorbents derived from agricultural waste, such as spent coffee grounds (SCGs), offers a promising alternative for removing humic acids and methyl orange (MO) dyes. These substances can clog reverse osmosis membranes, reduce the desalination efficiency during pretreatment and pose serious health risks. In this study, the properties and adsorption capacity of activated carbon (AC) produced from SCGs by chemical activation with H_3PO_4 were compared with those of commercial activated carbon (CAC). The adsorbent materials were characterized using SEM, FTIR, XRD and BET techniques, which revealed porous structures and functional groups beneficial for adsorption processes. The specific surface area of the SCG-derived activated carbon, determined by the BET method, was $520.40 \text{ m}^2/\text{g}$, indicating a substantial adsorption capacity. Under optimized conditions, the maximum adsorption of the MO on the PAC and crude SCG biosorbents reached 95.51% and 47.57%, respectively. Furthermore, the humic acid removal from seawater reached 60% with the PAC, compared with 55% with the CAC.

These findings indicate that the biosorbent (crude SCGs) was more effective at removing the MO dye than the HA from the seawater. The adsorption kinetic studies confirmed that the pseudo-second-order kinetic model and the Freundlich isotherm model best described the adsorption process for both the methyl orange and humic acid on the PAC adsorbent. These results suggest that valorizing coffee waste to produce activated carbon not only provides a sustainable waste recovery solution but also represents an environmentally friendly method for improving water treatment. The SCG-derived activated carbon shows great potential as a reusable bioadsorbent by positively impacting both the environment and treatment costs. Future research will focus on enhancing the adsorption characteristics of SCG-based activated carbon and demonstrating its scalability in commercial applications. The repurposing of spent coffee grounds for activated carbon production offers a sustainable approach to agricultural waste management, while producing materials with valuable properties for adsorption and other environmental technologies.

Author Contributions: Conceptualization, Z.T. and N.C.; methodology, Z.T., S.E.I.L. and L.M.; software, Z.T., O.B. and L.M.; validation, Z.T., S.E.I.L. and N.D.; formal analysis, Z.T., L.M. and N.A.A.; investigation, Z.T. and N.C.; resources, S.A., M.M. and D.T.; data curation, Z.T., O.B. and N.A.A.; writing—original draft preparation, Z.T.; writing—review and editing, Z.T., N.C., S.E.I.L. and N.D.; visualization, Z.T., N.C. and S.E.I.L.; supervision, Z.T. and S.E.I.L.; project administration, Z.T. and S.E.I.L. All authors have read and agreed to the published version of the manuscript.

Funding: This research received no external funding.

Institutional Review Board Statement: Not applicable.

Informed Consent Statement: Not applicable.

Data Availability Statement: The data presented in this study are available on request from the corresponding author.

Conflicts of Interest: The authors declare no conflicts of interest.

References

1. Idiz, E.F.; Carlisle, D.; Kaplan, I. Interaction between organic matter and trace metals in a uranium rich bog, Kern County, California, U.S.A. *Appl. Geochem.* **1986**, *1*, 573–590. [[CrossRef](#)]
2. Katsoyiannis, I.A.; Hug, S.J.; Ammann, A.; Zikoudi, A.; Hatziliontos, C. Arsenic speciation and uranium concentrations in drinking water supply wells in Northern Greece: Correlations with redox indicative parameters and implications for groundwater treatment. *Sci. Total. Environ.* **2007**, *383*, 128–140. [[CrossRef](#)] [[PubMed](#)]
3. Banning, A.; Benfer, M. Drinking Water Uranium and Potential Health Effects in the German Federal State of Bavaria. *Int. J. Environ. Res. Public Health* **2017**, *14*, 927. [[CrossRef](#)] [[PubMed](#)]
4. Crini, G. Non-conventional low-cost adsorbents for dye removal: A review. *Bioresour. Technol.* **2006**, *97*, 1061–1085. [[CrossRef](#)]
5. López, Y.C.; Ortega, G.A.; Reguera, E. Hazardous ions decontamination: From the element to the material. *Chem. Eng. J. Adv.* **2022**, *11*, 100297. [[CrossRef](#)]
6. Khan, S.; Naushad, M.; Govarthan, M.; Iqbal, J.; Alfadul, S.M. Emerging contaminants of high concern for the environment: Current trends and future research. *Environ. Res.* **2022**, *207*, 112609. [[CrossRef](#)]
7. Banat, I.M.; Nigam, P.; Singh, D.; Marchant, R. Microbial decolorization of textile-dyecontaining effluents: A review. *Bioresour. Technol.* **1996**, *58*, 217–227. [[CrossRef](#)]
8. Chatterjee, S.; Chatterjee, S.; Chatterjee, B.P.; Guha, A.K. Adsorptive removal of congo red, a carcinogenic textile dye by chitosan hydrobeads: Binding mechanism, equilibrium and kinetics. *Colloids Surf. A Physicochem. Eng. Asp.* **2007**, *299*, 146–152. [[CrossRef](#)]
9. Forgacs, E.; Cserhádi, T.; Oros, G. Removal of synthetic dyes from wastewaters: A review. *Environ. Int.* **2004**, *30*, 953–971. [[CrossRef](#)]
10. Robinson, T.; McMullan, G.; Marchant, R.; Nigam, P. Remediation of dyes in textile effluent: A critical review on current treatment technologies with a proposed alternative. *Bioresour. Technol.* **2001**, *77*, 247–255. [[CrossRef](#)]
11. Iwuozor, K.O.; Ighalo, J.O.; Emenike, E.C.; Ogunfowora, L.A.; Igwegbe, C.A. Adsorption of methyl orange: A review on adsorbent performance. *Curr. Res. Green Sustain. Chem.* **2021**, *4*, 100179. [[CrossRef](#)]
12. Albayati, T.M.; Alwan, G.M.; Mahdy, O.S. High performance methyl orange capture on magnetic nanoporous MCM-41 prepared by incipient wetness impregnation method. *Korean J. Chem. Eng.* **2017**, *34*, 259–265. [[CrossRef](#)]

13. Ali, I.; Burakova, I.; Galunin, E.; Burakov, A.; Mkrtychyan, E.; Melezhih, A.; Kurnosov, D.; Tkachev, A.; Grachev, V. High-Speed and High-Capacity Removal of Methyl Orange and Malachite Green in Water Using Newly Developed Mesoporous Carbon: Kinetic and Isotherm Studies. *ACS Omega* **2019**, *4*, 19293–19306. [[CrossRef](#)] [[PubMed](#)]
14. Elgarahy, A.M.; Elwakeel, K.Z.; Mohammad, S.H.; Elshoubaky, G.A. A critical review of biosorption of dyes, heavy metals and metalloids from wastewater as an efficient and green process. *Clean. Eng. Technol.* **2021**, *4*, 100209. [[CrossRef](#)]
15. Jawad, A.H.; Kadhum, A.M.; Ngoh, Y. Applicability of dragon fruit (*Hylocereus polyrhizus*) peels as low-cost biosorbent for adsorption of methylene blue from aqueous solution: Kinetics, equilibrium and thermodynamics studies. *Desalination Water Treat.* **2018**, *109*, 231–240. [[CrossRef](#)]
16. Maheshwari, U.; Thakur, R.V.; Deshpande, D.; Ghodke, S. Efficiency evaluation of orange and banana peels for dye removal from synthetic industrial effluent. *Mater. Today Proc.* **2023**, *76*, 170–176. [[CrossRef](#)]
17. Bhatti, H.N.; Sadaf, S.; Naz, M.; Iqbal, M.; Safa, Y.; Ain, H.; Nawaz, S.; Nazir, A. Enhanced adsorption of Foron Black RD 3GRN dye onto sugarcane bagasse biomass and Na-alginate composite. *Desalination Water Treat.* **2021**, *216*, 423–435. [[CrossRef](#)]
18. Elsayed, A.E.; Osman, D.I.; Attia, S.K.; Ahmed, H.M.; Shoukry, E.M.; Mostafa, Y.M.; Taman, A.R. A Study on the removal characteristics of organic and inorganic pollutants from wastewater by low cost biosorbent. *Egypt. J. Chem.* **2019**, *63*, 1429–1442. [[CrossRef](#)]
19. Tee, G.T.; Gok, X.Y.; Yong, W.F. Adsorption of pollutants in wastewater via biosorbents, nanoparticles and magnetic biosorbents: A review. *Environ. Res.* **2022**, *212*, 113248. [[CrossRef](#)]
20. Ozdemir, N.C.; Bilici, Z.; Yabalak, E.; Dizge, N.; Balakrishnan, D.; Khoo, K.S.; Show, P.L. Physico-chemical adsorption of cationic dyes using adsorbent synthesis via hydrochloric acid treatment and subcritical method from palm leaf biomass waste. *Chemosphere* **2023**, *339*, 139558. [[CrossRef](#)]
21. Athira, T.M.; Sumi, S. Agro-based Adsorbents for Dye Removal from Aqueous Solutions: A Review. *Water Air, Soil Pollut.* **2024**, *235*, 120. [[CrossRef](#)]
22. Abu Hassan, N.H.; Adenan, N.H. Influence of pre-treated local fruit peels in remediating dye pollutant. *Mater. Today Proc.* **2023**, *88*, 10–14. [[CrossRef](#)]
23. Dey, S.; Basha, S.; Babu, G.; Nagendra, T. Characteristic and biosorption capacities of orange peels biosorbents for removal of ammonia and nitrate from contaminated water. *Clean. Mater.* **2021**, *1*, 100001. [[CrossRef](#)]
24. Solih, F.A.; Buthiyappan, A.; Hasikin, K.; Aung, K.M.; Raman, A.A.A. Optimization-driven modelling of hydrochar derived from fruit waste for adsorption performance evaluation using response surface methodology and machine learning. *J. Ind. Eng. Chem.* **2024**. [[CrossRef](#)]
25. Ogunlalu, O.; Oyekunle, I.P.; Iwuozor, K.O.; Aderibigbe, A.D.; Emenike, E.C. Trends in the mitigation of heavy metal ions from aqueous solutions using unmodified and chemically-modified agricultural waste adsorbents. *Curr. Res. Green Sustain. Chem.* **2021**, *4*, 100188. [[CrossRef](#)]
26. Vakili, A.; Zinatizadeh, A.; Rahimi, Z.; Zinadini, S.; Mohammadi, P.; Azizi, S.; Karami, A.; Abdulgader, M. The impact of activation temperature and time on the characteristics and performance of agricultural waste-based activated carbons for removing dye and residual COD from wastewater. *J. Clean. Prod.* **2023**, *382*, 134899. [[CrossRef](#)]
27. Kainth, S.; Sharma, P.; Pandey, O. Green sorbents from agricultural wastes: A review of sustainable adsorption materials. *Appl. Surf. Sci. Adv.* **2024**, *19*, 100562. [[CrossRef](#)]
28. Tramontin, D.P.; Cadena-Carrera, S.E.; Bella-Cruz, A.; Cruz, C.C.B.; Bolzan, A.; Quadri, M.B. Biological activity and chemical profile of Brazilian jackfruit seed extracts obtained by supercritical CO₂ and low pressure techniques. *J. Supercrit. Fluids* **2019**, *152*, 104551. [[CrossRef](#)]
29. Yorgun, S.; Yıldız, D. Preparation and characterization of activated carbons from Paulownia wood by chemical activation with H₃PO₄. *J. Taiwan Inst. Chem. Eng.* **2015**, *53*, 122–131. [[CrossRef](#)]
30. Prahas, D.; Kartika, Y.; Indraswati, N.; Ismadji, S. Activated carbon from jackfruit peel waste by H₃PO₄ chemical activation: Pore structure and surface chemistry characterization. *Chem. Eng. J.* **2008**, *140*, 32–42. [[CrossRef](#)]
31. Djilani, C.; Zaghoudi, R.; Djazi, F.; Bouchekima, B.; Lallam, A.; Modarressi, A.; Rogalski, M. Adsorption of dyes on activated carbon prepared from apricot stones and commercial activated carbon. *J. Taiwan Inst. Chem. Eng.* **2015**, *53*, 112–121. [[CrossRef](#)]
32. Bourafa, A.; Berrich, E.; Belhachemi, M.; Jellali, S.; Jeguirim, M. Preparation and characterization of hydrochars and CO₂-activated hydrochars from date and olive stones. *Biomass-Convert. Biorefin.* **2024**, *14*, 20385–20396. [[CrossRef](#)]
33. Zhang, L.; Liu, S.; Wang, B.; Wang, Q.; Yang, G.; Chen, J. Effect of Residence Time on Hydrothermal Carbonization of Corn Cob Residual. *BioResources* **2015**, *10*, 3979–3986. [[CrossRef](#)]
34. Xu, J.; Liu, J.; Ling, P.; Zhang, X.; Xu, K.; He, L.; Wang, Y.; Su, S.; Hu, S.; Xiang, J. Raman spectroscopy of biochar from the pyrolysis of three typical Chinese biomasses: A novel method for rapidly evaluating the biochar property. *Energy* **2020**, *202*, 117644. [[CrossRef](#)]
35. Tiegam, R.F.T.; Tchuiwon, D.R.T.; Santagata, R.; Nanssou, P.A.K.; Anagho, S.G.; Ionel, I.; Ulgiati, S. Production of activated carbon from cocoa pods: Investigating benefits and environmental impacts through analytical chemistry techniques and life cycle assessment. *J. Clean. Prod.* **2021**, *288*, 125464. [[CrossRef](#)]

36. Foo, K.; Hameed, B. Coconut husk derived activated carbon via microwave induced activation: Effects of activation agents, preparation parameters and adsorption performance. *Chem. Eng. J.* **2012**, *184*, 57–65. [[CrossRef](#)]
37. Bergna, D.; Varila, T.; Romar, H.; Lassi, U. Activated carbon from hydrolysis lignin: Effect of activation method on carbon properties. *Biomass-Bioenergy* **2022**, *159*, 106387. [[CrossRef](#)]
38. Zakaria, M.R.; Farid, M.A.A.; Andou, Y.; Ramli, I.; Hassan, M.A. Production of biochar and activated carbon from oil palm biomass: Current status, prospects, and challenges. *Ind. Crops Prod.* **2023**, *199*, 116767. [[CrossRef](#)]
39. Deng, S.; Hu, B.; Chen, T.; Wang, B.; Huang, J.; Wang, Y.; Yu, G. Activated carbons prepared from peanut shell and sunflower seed shell for high CO₂ adsorption. *Adsorption* **2015**, *21*, 125–133. [[CrossRef](#)]
40. Ghosh, R.K.; Debnath, S.; Ray, D.P. Carbonized jute agrowaste—A sustainable resource for wastewater treatment. In *Sustainable Technologies for Textile Wastewater Treatments*; Elsevier: Amsterdam, The Netherlands, 2021; pp. 67–94. [[CrossRef](#)]
41. Zhang, B.; Jiang, Y.; Balasubramanian, R. Synthesis, formation mechanisms and applications of biomass-derived carbonaceous materials: A critical review. *J. Mater. Chem. A* **2021**, *9*, 24759–24802. [[CrossRef](#)]
42. Ching, S.L.; Yousoff, M.S.; Aziz, H.A.; Umar, M. Influence of impregnation ratio on coffee ground activated carbon as landfill leachate adsorbent for removal of total iron and orthophosphate. *Desalination* **2011**, *279*, 225–234. [[CrossRef](#)]
43. Kante, K.; Nieto-Delgado, C.; Rangel-Mendez, J.R.; Badosz, T.J. Spent coffee-based activated carbon: Specific surface features and their importance for H₂S separation process. *J. Hazard. Mater.* **2012**, *201–202*, 141–147. [[CrossRef](#)]
44. Wang, C.-H.; Wen, W.-C.; Hsu, H.-C.; Yao, B.-Y. High-capacitance KOH-activated nitrogen-containing porous carbon material from waste coffee grounds in supercapacitor. *Adv. Powder Technol.* **2016**, *27*, 1387–1395. [[CrossRef](#)]
45. Laksaci, H.; Khelifi, A.; Trari, M.; Addoun, A. Synthesis and characterization of microporous activated carbon from coffee grounds using potassium hydroxides. *J. Clean. Prod.* **2017**, *147*, 254–262. [[CrossRef](#)]
46. Anastopoulos, I.; Karamesouti, M.; Mitropoulos, A.C.; Kyzas, G.Z. A review for coffee adsorbents. *J. Mol. Liq.* **2017**, *229*, 555–565. [[CrossRef](#)]
47. Boudrahem, F.; Aissani-Benissad, F.; Aït-Amar, H. Batch sorption dynamics and equilibrium for the removal of lead ions from aqueous phase using activated carbon developed from coffee residue activated with zinc chloride. *J. Environ. Manag.* **2009**, *90*, 3031–3039. [[CrossRef](#)]
48. Laksaci, H.; Khelifi, A.; Belhamdi, B.; Trari, M. Valorization of coffee grounds into activated carbon using physic—Chemical activation by KOH/CO₂. *J. Environ. Chem. Eng.* **2017**, *5*, 5061–5066. [[CrossRef](#)]
49. Babu, A.N.; Reddy, D.S.; Kumar, G.S.; Ravindhranath, K.; Mohan, G.K. Removal of lead and fluoride from contaminated water using exhausted coffee grounds based bio-sorbent. *J. Environ. Manag.* **2018**, *218*, 602–612. [[CrossRef](#)]
50. Bergamini, M.H.L.; de Oliveira, S.B.; Scalize, P.S. Production of activated carbon from exhausted coffee grounds chemically modified with natural eucalyptus ash lye and its use in the fluoride adsorption process. *Environ. Sci. Pollut. Res.* **2023**, *30*, 91276–91291. [[CrossRef](#)] [[PubMed](#)]
51. Pelekani, C.; Snoeyink, V.L. Competitive adsorption between atrazine and methylene blue on activated carbon: The importance of pore size distribution. *Carbon* **2000**, *38*, 1423–1436. [[CrossRef](#)]
52. Tran, T.H.; Le, A.H.; Pham, T.H.; Nguyen, D.T.; Chang, S.W.; Chung, W.J. Adsorption isotherms and kinetic modeling of methylene blue dye onto a carbonaceous hydrochar adsorbent derived from coffee husk waste. *Sci. Total. Environ.* **2020**, *725*, 138325. [[CrossRef](#)]
53. Jung, K.-W.; Choi, B.H.; Hwang, M.-J.; Jeong, T.-U.; Ahn, K.-H. Fabrication of granular activated carbons derived from spent coffee grounds by entrapment in calcium alginate beads for adsorption of acid orange 7 and methylene blue. *Bioresour. Technol.* **2016**, *219*, 185–195. [[CrossRef](#)]
54. Rosson, E.; Garbo, F.; Marangoni, G.; Bertani, R.; Lavagnolo, M.C.; Moretti, E.; Talon, A.; Mozzon, M.; Sgarbossa, P. Activated Carbon from Spent Coffee Grounds: A Good Competitor of Commercial Carbons for Water Decontamination. *Appl. Sci.* **2020**, *10*, 5598. [[CrossRef](#)]
55. Popovici, D.; Dutescu, C.; Neagu, M. Removal of phenol from aqueous solutions on activated carbon obtained from coffee grounds. *Rev. Chim* **2016**, *67*, 751–756.
56. Zermane, F.; Naceur, M.; Cheknane, B.; Messaoudene, N.A. Adsorption of humic acids by a modified Algerian montmorillonite in synthesized seawater. *Desalination* **2005**, *179*, 375–380. [[CrossRef](#)]
57. Yazza, N.; Rouan, F.; Tigrine, Z. Préparation et Caractérisation d'un Charbon actif à Base d'un Déchet de Café pour le Prétraitement des Eaux. Master's Thesis, Université Blida, Blida, Algeria, 2022.
58. Mitra, S.; Mukherjee, T.; Kaparaju, P. Prediction of methyl orange removal by iron decorated activated carbon using an artificial neural network. *Environ. Technol.* **2021**, *42*, 3288–3303. [[CrossRef](#)]
59. El Maguana, Y.; Elhadiri, N.; Bouchdoug, M.; Benchanaa, M.; Jaouad, A. Activated Carbon from Prickly Pear Seed Cake: Optimization of Preparation Conditions Using Experimental Design and Its Application in Dye Removal. *Int. J. Chem. Eng.* **2019**, *2019*, 1–12. [[CrossRef](#)]
60. Islam, T.; Saenz-Arana, R.; Hernandez, C.; Guinto, T.; Ahsan, A.; Bragg, D.T.; Wang, H.; Alvarado-Tenorio, B.; Noveron, J.C. Conversion of waste tire rubber into a high-capacity adsorbent for the removal of methylene blue, methyl orange, and tetracycline from water. *J. Environ. Chem. Eng.* **2018**, *6*, 3070–3082. [[CrossRef](#)]

61. Yu, Y.; Qiao, N.; Wang, D.; Zhu, Q.; Fu, F.; Cao, R.; Wang, R.; Liu, W.; Xu, B. Fluffy honeycomb-like activated carbon from popcorn with high surface area and well-developed porosity for ultra-high efficiency adsorption of organic dyes. *Bioresour. Technol.* **2019**, *285*, 121340. [[CrossRef](#)] [[PubMed](#)]
62. Rattanapan, S.; Srikram, J.; Kongsune, P. Adsorption of Methyl Orange on Coffee grounds Activated Carbon. *Energy Procedia* **2017**, *138*, 949–954. [[CrossRef](#)]

Disclaimer/Publisher's Note: The statements, opinions and data contained in all publications are solely those of the individual author(s) and contributor(s) and not of MDPI and/or the editor(s). MDPI and/or the editor(s) disclaim responsibility for any injury to people or property resulting from any ideas, methods, instructions or products referred to in the content.